International Journal of Advanced Technology in Engineering and Science
Vol. No.4, Issue No. 01, January 2016
www.ijates.com
ijates
ISSN 2348 - 7550

MICROMECHANICS OF THERMOELASTIC BEHAVIOR OF AA2024/MgO METAL MATRIX COMPOSITES

Chennakesava R Alavala

Department of Mechanical Engineering, JNT University, Hyderabad, (India)

ABSTRACT

The present work was intended to estimate thermoelastic behavior of AA2024/magnesium oxide nanoparticle metal matrix composites. The RVE models were used to analyze thermo-elastic behavior. The stiffness of AA2024/ magnesium oxide nanoparticle metal matrix composites decreased with the increase of temperature. Below 0^{o}C and above 100^{o}C MgO nanoparticles were fractured except in range of 0^{o}C to 100^{o}C where the interphase has fractured.

Keywords: AA2024 alloy, magnesium oxide, RVE model, thermoelastic, finite element analysis.

I. INTRODUCTION

The exploit of reinforcing particulates as stiffening agents in the metal matrix composites has received considerable attention for variety of applications. Aluminum alloys are valued for comprising low density and high ductility, but they lack the strength and stiffness. By reinforcing an aluminum alloy with nanoparticulates of stronger and stiffer material such as SiC [1-5], alumina [6-10], alumina trihydrate [11] or carbon [12], it is achievable to fabricate a composite that preserves the light weight of the aluminum alloy while attaining greater strength and stiffness. Apart from Al-alloys and Mg-alloys [13] are widely suitable as matrix materials in the metal matrix composites wished-for for automotive applications.

Thermal stability of the nanoparticulates and matrix materials is exceptionally essential to appraise the suitability of these materials in diverse applications. Thermal decomposition kinetics and interaction of thermal energy between particulate and matrix are imperative for sustainability of metal matrix composites for high temperature purposes [14, 15]. For instance, acquaintance of the coefficient of thermal friction (CTE) of metal matrix composites is obligatory in computing dimensional changes and induced internal stresses when composites are suffered to temperature changes.

Magnesium oxide (MgO) has elastic modulus of approximately 300 GPa, shear modulus of 122 GPa and CTE (coefficient of thermal expansion) of 12 µm/m-^{o}C. The MgO nanoparticles have high surface reactivity and high chemical and thermal stability, which make MgO a hopeful material for applications in fields of sensors, semiconductors, etc. AA2024 alloy has elastic modulus of 71.7 GPa, shear modulus of 26 GPa and CTE of 7.4 µm/m-^{o}C. AA 2024 alloy is used for motorbike or bicycle frames and armored vehicles.

The present work was planned to investigate the thermoelastic behavior of nanoparticulate MgO/AA2024 alloy matrix composites. Finite element analysis (FEA) was implemented to measure the local response of the material using representative volume element (RVE) reinforced by a single particle subjected to hydrostatic and isothermal loading.

Table 1. Mechanical properties of AA2024 matrix and MgO nanoparticles.

Property	AA2024	MgO
Density, g/cc	2.78	3.54
Elastic modulus, GPa	73.1	330
Ultimate tensile strength, MPa	395	166
Poisson's ratio	0.33	0.35
CTE, µm/m-^{o}C	21.1	12.0
Thermal Conductivity, W/m-K	121.0	60.0
Specific heat, J/kg-K	875	1030

II. MATERIAL AND METHODS

The matrix material was AA2024 alloy. The reinforcement nanoparticulate was MgO of average size 100nm. The mechanical properties of materials used in the current work are given in table 1. The volume fractions of MgO nanoparticles were 20% and 30%. In this investigation, a square RVE (Fig. 1) was outfitted to interpret the thermo-elastic (compressive) behavior AA2024/MgO nanocomposites. The PLANE183 element was used in the matrix and the interphase regions in the RVE models. The interphase between nanoparticle and matrix was discretized with CONTACT172 element [16]. The maximum contact friction stress of $\sigma_y/\sqrt{3}$ (where, σ_y is the yield stress of the material being deformed) was enforced at the contact surface. Both uniform thermal and hydrostatic pressure loads were applied simultaneously on the RVE model.

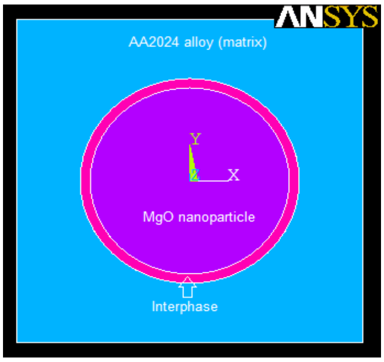

Fig. 1. The RVE model.

Poisson's ratio can have positive or negative values of large magnitude in anisotropic materials. For orthotropic materials, Poisson's ratio is bounded by the ratio of Young's moduli E as follows [17, 18]:

$$|v_{12}| < (E_x / E_y)^{1/2} \quad (1)$$

The other definition of major Poisson's ratio is as follows:

$$|v_{12}| = -\varepsilon_y / \varepsilon_x \tag{2}$$

In the present work, Poisson's ratio v_{12} was calculated to validate the results.

III. RESULTS AND DISCUSSION

The finite element analysis (FEA) was carried out at -100°C to 300°C isothermal conditions. The hydrostatic pressure load was applied RVE model to investigate micromechanics thermo-elastic tensile behavior of AA2024/MgO nanoparticulate composites. The volume fractions of MgO nanoparticles in the AA2024 matrix were 10% and 30%.

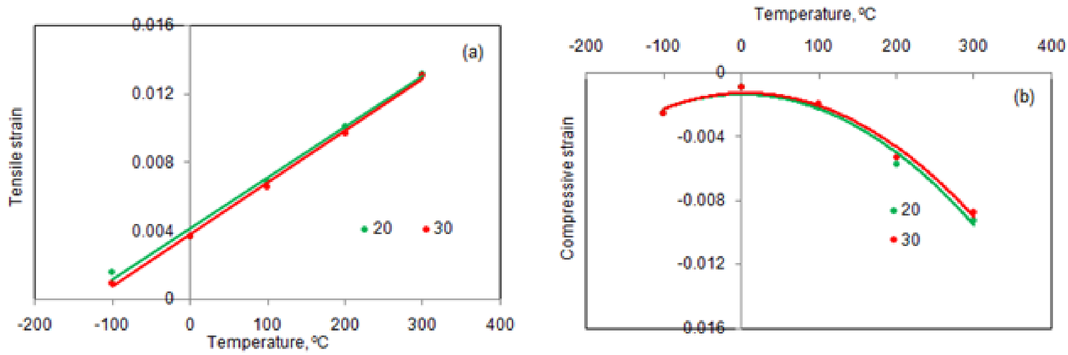

Fig. 2. Influence of temperature on thermoelastic strain.

3.1 Micromechanics of Thermo-Elastic Behavior

Thermo-elastic strains as a function of temperature are showed in Fig. 2. The increase of temperature increased the tensile strains along the load direction while the compressive strains along the transverse direction decreased. In the composites having low volume fraction (20%) of MgO nanoparticles, the matrix (AA2024 alloy) had experienced the large tensile strains as the temperature changed from -100°C to 300°C temperature as showed in Fig. 3(a). The MgO nanoparticle had experienced the compressive strains for the temperature loading of -100°C and 0°C, while the interphase experienced the compressive strains for temperature loading from -100°C to 300°C as shown in Fig. 3(b). The same kind of trend was observed in the composites having high volume fraction (30%) of MgO nanoparticles (Fig. 4). The strains were higher in the composites comprising low volume fraction of MgO than those induced in the composites comprising high volume fraction of MgO as revealed in Figs. 2, 3 and 4. The behavior of tensile strains was linear and it was quadratic for the compressive strains. Tensile and compressive strengths as a function of temperature is depicted in Fig. 5. The tensile strength increased with the increase of temperature as showed in Fig. 5(a). The tensile strength deteriorated with increase in the volume fraction of MgO. This is due to fact that the tensile strength of AA2024 matrix alloy and MgO nanoparticles are, respectively, 395 MPa and 166 MPa. The compressive strength decreased with increase of temperature from -100°C to 100°C and later on it was increased from temperature change from 100°C to 300°C as showed in Fig. 5(b).

International Journal of Advanced Technology in Engineering and Science
Vol. No.4, Issue No. 01, January 2016
www.ijates.com
ijates
ISSN 2348 - 7550

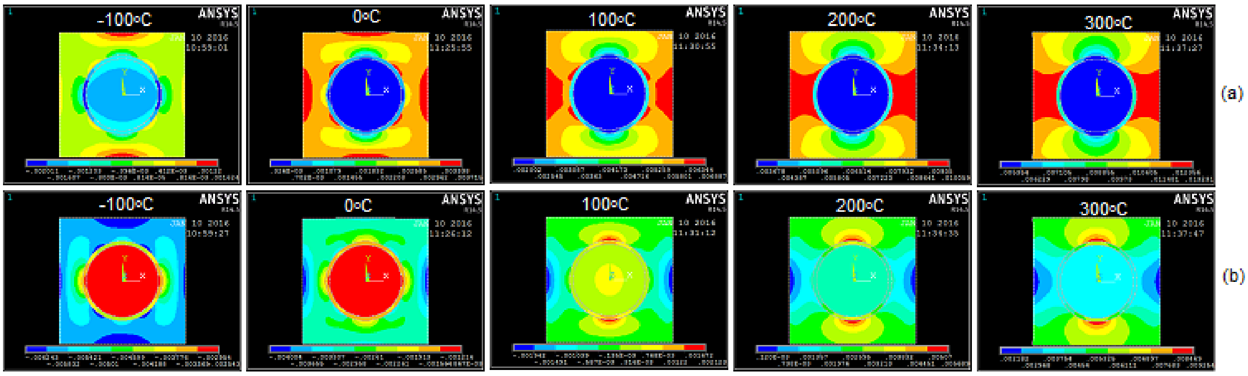

Fig.3. Raster images of tensile strains of AA2024/20%MgO composites: (a) Tensile and (b) Compression.

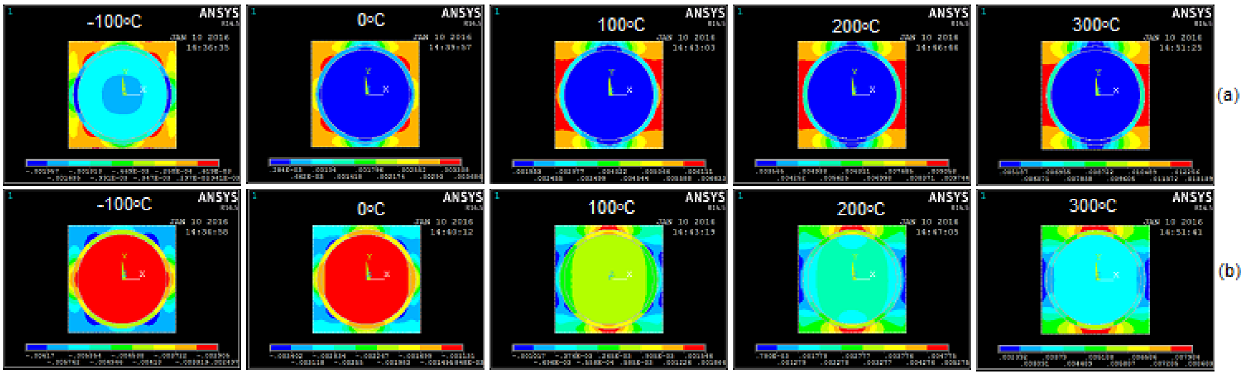

Fig. 4. Raster images of compressive strains of AA2024/30% MgO composites.

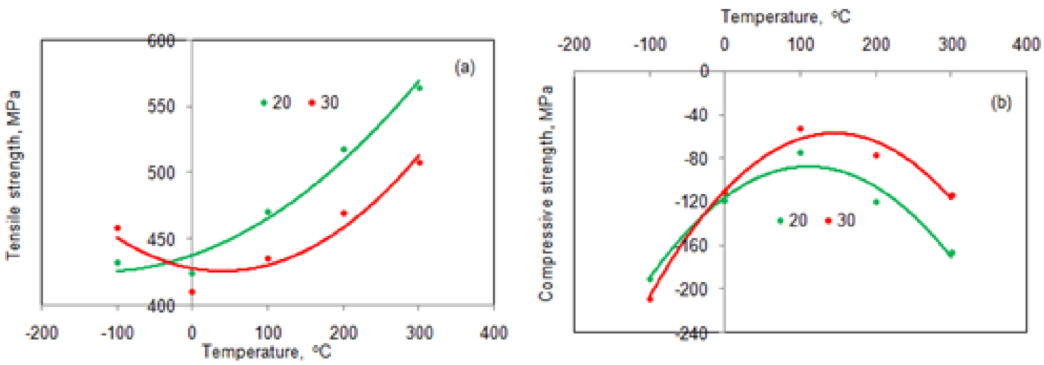

Fig. 5. Influence of temperature on strength.

Fig. 6 and 7 show raster images of stresses induced in the composites having 20% MgO and 30%MgO nanoparticles, respectively. The orientation of tensile stresses were along the direction of loading as showed in Figs. 6(a) and 7(a) whereas it was in the transverse direction of tensile loading as showed in Figs. 6(b) and 7(b). The transfer of stresses increased with the increase of temperature from the matrix to the nanoparticle as seen from the order of colors. It is also observed that the nanoparticles had experienced different local stress fields as indicated by the spectrum of different colors bands in the particles. The MgO nanoparticles are heavily loaded (high stress color bands such as red). This is because of the lower threshold value (low tensile strength of 166

ijates
ISSN 2348 - 7550

MPa) of MgO nanoparticles. As the temperature increases the maximum stress band propagates from the matrix to the centre of the MgO nanoparticle through the interphase.

The tensile elastic modulus along x-direction decreased with the increase of temperature as showed in Fig. 8(a). This kind of phenomena was also observed in [19] and [20]. The compressive elastic modulus along y-direction increased initially from -100°C to 0°C and later on it decreased from 0oC to 300°C. The tensile elastic modulus was very high below 0°C whereas the compressive elastic modulus was low below 0°C. The MgO nanoparticles are very stiffer to undergo deformation under tensile loading while they undergo shortening at very low temperatures. This phenomenon is also confirmed with the variation of major Poisson's ration with the temperature (Fig. 9). Poisson's ratio is bounded by the ratio of Young's moduli E as mentioned in Eq. (1).

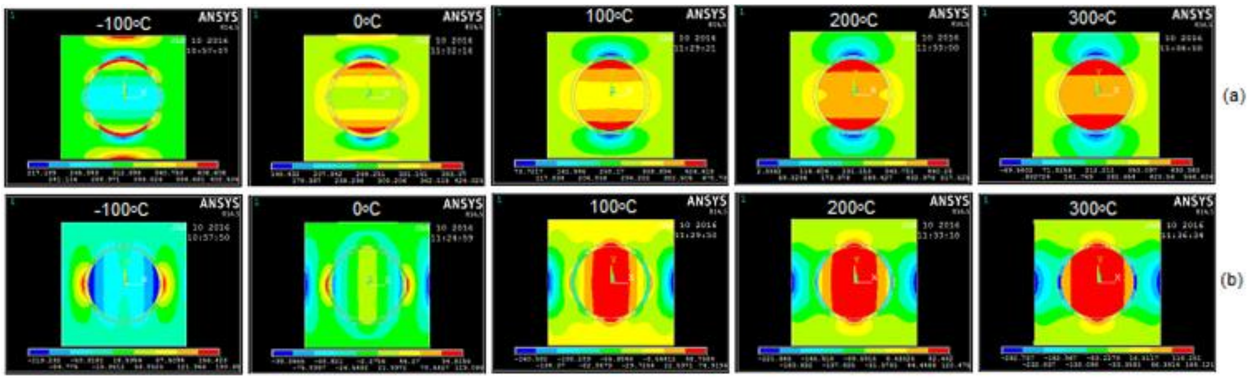

Fig. 6. Raster images of tensile and compressive stresses of AA2024/20% MgO composites.

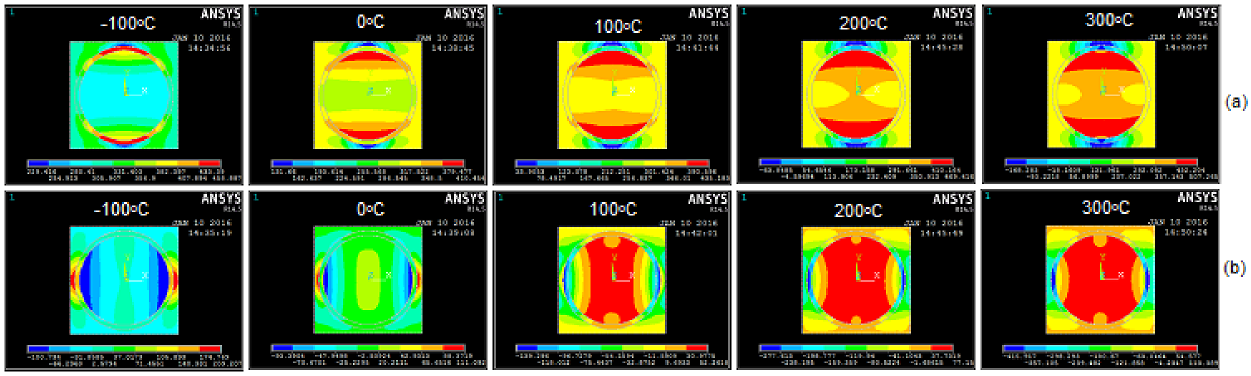

Fig. 7. Raster images of tensile and compressive stresses of AA2024/30% MgO composites.

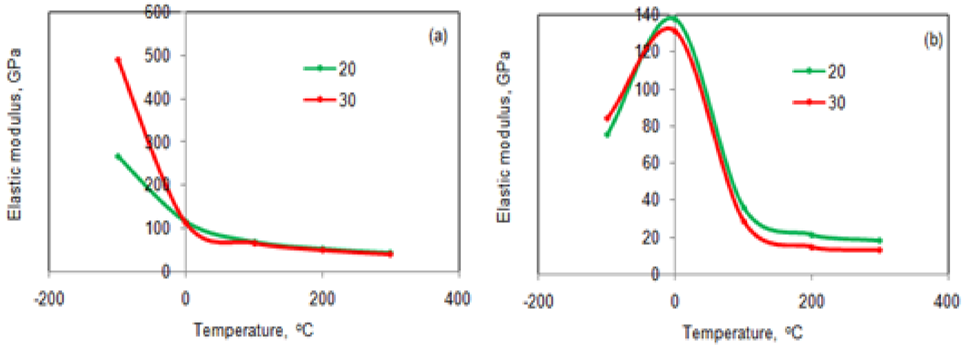

Fig. 8. Influence of temperature on elastic modulus: (a) E_x and (b) E_y.

ijates
ISSN 2348 - 7550

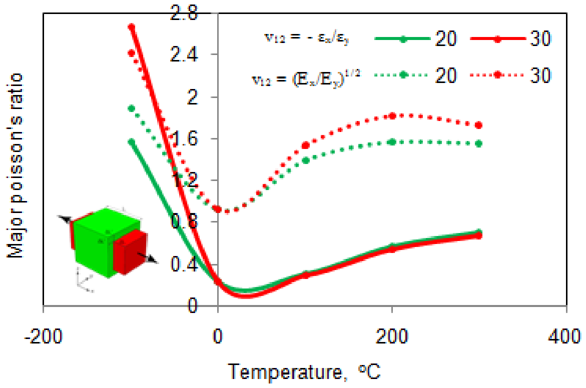

Fig. 9. Influence of temperature on major Poisson's ratio.

3.2 Fracture Behavior

Fig. 10 describes the von Mises stress induced in the composites. The von Mises stress decreased with the increase of temperature from -100°C to 0°C and later it increased with the increase of temperature. The von Mises stress was higher in the composites having 20% MgO nanoparticles than that in the composites consisting of 30% MgO. Below 0°C and above 100°C MgO nanoparticles (Fig. 11) were fractured except in range of 0°C to 100°C where the interphase has fractured. This indicates that AA2024/MgO nanoparticulate metal matrix composites are not suitable for the applications below 0°C and above 100°C temperatures. The damage of MgO nanoparticle is illustrated in Fig. 12. Multidirectional cracks are seen in the MgO nanoparticle representing the multi local stress fields.

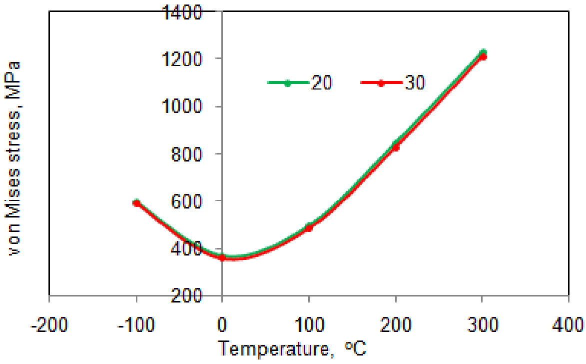

Fig. 10. Influence of temperature on von Mises stress.

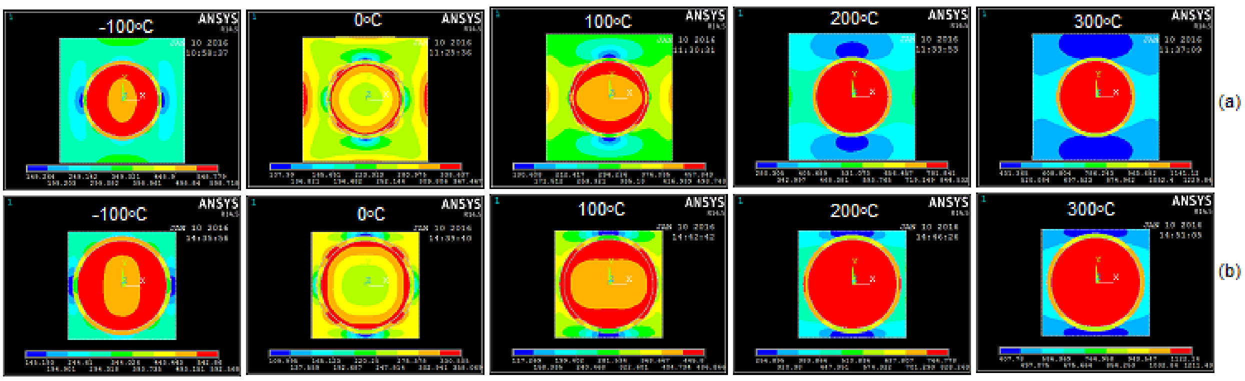

Fig. 11. Raster images of von Mises stress of AA2024/MgO composites: (a) 20% MgO and (b) 30% MgO.

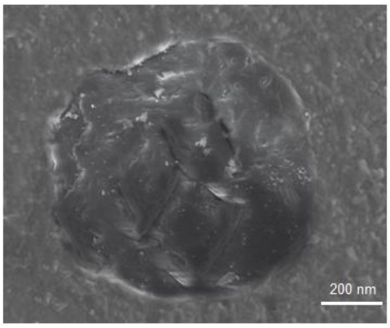

Fig. 12. SEM image illustrating damage of MgO nanoparticle.

IV. CONCLUSIONS

The tensile elastic strains increased with the increase of temperature. The tensile strength increased with the increase of temperature. Interestingly, the stiffness decreased with increase of temperature for AA2024/MgO nanoparticulate metal matrix composites. Below 0^oC and above 100^oC MgO nanoparticles were fractured except in range of 0^oC to 100^oC where the interphase has fractured.

REFERENCES

[1] C. Reddy and B. Kotiveerachari, Effect of Matrix Microstructure and Reinforcement Fracture on the Properties of Tempered SiC/Al-Alloy Composites, National conference on advances in materials and their processing, Bagalkot, 28-29th November, 2003, 78-81.

[2] S. Sujatha and A. C. Reddy, Assessment of strength improvement in heat treated AA2024/SiC metal matrix composites using finite element analysis: experimental validation, National Conference on Advances in Design Approaches and Production Technologies (ADAPT-2005), Hyderabad, 22-23rd August 2005, 341-343.

[3] M. Chamundeswari and A. C. Reddy, Evaluation of strength improvement in tempered AA5050/SiC metal matrix composites using finite element analysis: experimental validation, National Conference on Advances in Design Approaches and Production Technologies (ADAPT-2005), Hyderabad, 22-23rd August 2005, 338-340.

[4] A. C. Reddy, Mechanical properties and fracture behavior of 6061/SiCp Metal Matrix Composites Fabricated by Low Pressure Die Casting Process, Journal of Manufacturing Technology Research, 1(3&4), 2009, 273-286.

[5] C. Reddy, Tensile fracture behavior of 7072/SiCp metal matrix composites fabricated by gravity die casting process, Materials Technology: Advanced Performance Materials, 26(5), 2011, 257-262.

[6] K. Swapna Sudha and A. C. Reddy, Tensile performance of heat treated AA2024/Al_2O_3 metal matrix composites using RVE models: experimental validation, National Conference on Advances in Design Approaches and Production Technologies (ADAPT-2005), Hyderabad, 22-23rd August 2005, 332-334.

[7] V. K. Prasad and A. C. Reddy, Tensile behavior of tempered AA5050/Al_2O_3 metal matrix composites using RVE models: experimental validation, National Conference on Advances in Design Approaches and Production Technologies (ADAPT-2005), Hyderabad, 22-23rd August 2005, 335-337.

[8] A. C. Reddy and Essa Zitoun, Tensile properties and fracture behavior of 6061/Al_2O_3 metal matrix composites fabricated by low pressure die casting process, International Journal of Materials Sciences, 6(2), 2011, 147-157.

[9] A. C. Reddy and Essa Zitoun, Tensile behavior 0f 6063/Al_2O_3 particulate metal matrix composites fabricated by investment casting process, International Journal of Applied Engineering Research, 1(3), 2010, 542-552.

[10] A. C. Reddy and Essa Zitoun, Matrix al-alloys for alumina particle reinforced metal matrix composites, Indian Foundry Journal, 55(1), 2009, 12-16.

[11] C. Reddy, Studies on fracture behavior of brittle matrix and alumina trihydrate particulate composites, Indian Journal of Engineering & Materials Sciences, 9(5), 2003, 365-368.

[12] C. Reddy, Analysis of the Relationship Between the Interface Structure and the Strength of Carbon-Aluminum Composites, NATCON-ME, Bangalore, 13-14th March 2004, 61-62.

[13] Ramana A. C. Reddy, and S. S. Reddy, Fracture analysis of mg-alloy metal matrix composites, National Conference on Computer Applications in mechanical Engineering, Anantapur, 21st December 2005, 57-61.

[14] E. Carreno, S.E. Urreta and R. Schaller, Mechanical spectroscopy of thermal stress relaxation at metal-ceramic interfaces in Aluminum-based composites, Acta Materialia, 48, (2000), 4725-4733.

[15] A. C. Reddy and B. Kotiveerachari, Effect of aging condition on structure and the properties of Al-alloy / SiC composite, International Journal of Engineering and Technology, 2(6), 2010, 462-465.

[16] C.R. Alavala, Finite element Mehods: basic Concepts and Applications, PHI Learning Pvt. Ltd., New Dlehi, 2008.

[17] M. Lempriere Poisson's ratio in orthotropic materials, AIAA Journal, 6(11), 1968, 2226-2227.

[18] A. C. Reddy, Experimental Evaluation of Elastic Lattice Strains in the Discontinuously SiC Reinforced Al-alloy Composites, National Conference on Emerging Trends in Mechanical Engineering, Nagpur, 5-6th February, 2004, 81.

[19] Duschlbauer, H.J. Bohm and H.E. Pettermann, Computational simulation of composites reinforced by planar random fibers: Homogenization and localization by unit cell and mean field approaches, Journal of Composite Materials, 40, 2006, 2217–2234.

[20] Doghri and C.Friebel, Effective elasto-plastic properties of inclusion reinforced composites. Study of shape, orientation and cyclic response, Mechanics of Materials, 37, 2005, 45–68.